International Conference on Space Optics—ICSO 1997

Toulouse, France

2–4 December 1997

Edited by George Otrio

Optimized technical and scientific design approach for high performance anticoincidence shields

Roland Graue, Timo Stuffler, Franco Monzani, Paolo Bastia, et al.

International Conference on Space Optics — ICSO 1997, edited by Georges Otrio, Proc. of SPIE Vol. 10570, 1057011 · © 1997 ESA and CNES · CCC code: 0277-786X/18/$18 · doi: 10.1117/12.2326475

Optimized Technical and Scientific Design Approach for High Performance Anticoincidence Shields

Roland GRAUE*, Timo STUFFLER*, Franco MONZANI°, Paolo BASTIA°, Werner GRYKSA' Germit PAHL'

**Kayser-Threde GmbH, Munich;°Laben S.p.A., Vimodrone (Milano);*
'CASE GmbH, Munich

ABSTRACT - *Scintillation detectors are widely used for the detection of astronomical Gamma-Rays in the energy range between 50 keV up to 10 MeV. The powerful Anticoincidence Shields for the INTEGRAL core instruments - Imager and Spectrometer generate the FOV of the dedicated core detectors (CdTe/CsI, Germanium) by passive blocking (absorption) and beyond a definite threshold level by active suppression (i.e. generation of a fast veto signal for the Imager and Spectrometer electronics) of the cosmic and self induced diffuse and γ - and x-ray radiation environment. Minimized ACS shield leakage and small FOV of the instruments request large and heavy, anticoincidence shields mainly based on BGO or CsI crystal slabs in combination with ultra sensitive PMT pairs on each detector module enabling even single photon counting.*

The sophisticated design approach for the INTEGRAL SPI ACS as a strategy for a streamlined development of future complex and cost effective ACS systems is described. The design approach represents an improved concept of the INTEGRAL Phase B set-up. Main emphasis in our concept is given to describe the isostatic suspension of the very brittle BGO crystal material using very stiff honeycomb substructures with adapted material properties and the optimized electronic architecture with modular front end electronic and with several high voltage power supplies dedicated to detector module clusters derived from the SAX [1] program. Minimized power consumption, enhanced low noise behavior, improved detector chain timing strategy for a reduction of the adaptive spectrometer dead time and functional single point failure redundancy is highlighted. Additionally, an innovative multi layer coating of the crystals offers significantly higher Light Collection Efficiency of the detector units and therefore an improved SNR performance. On flight diagnostics of the detector chain life time degradation can be performed by pulse height analysis, using natural (e.g. background radiation) sources and by implemented pulse generators (multivibrator) driving LED sources placed in the PMT FOV.

1 - INTRODUCTION

The INTEGRAL Spectrometer Anticoincidence system (ACS) consists of 2 rings (Upper Collimator, Lower Collimator), 2 shields (Upper Side, Lower Side) with hexagonal shape, and the Rear Shield. The crystal material is BGO. For the active detection of scintillation light induced through gamma-rays in the 90 crystal segments, 162 1.5 inch PMT's are mounted at different locations of the ACS. For reasons of redundancy two PMT's look into the same crystal segment (except for the Upper Collimator Ring) and for the generation of the Veto signal the sum signal of both PMT's is used.

2 - TECHNICAL APPROACH

2.1 - Main Structure

High thermal stresses occur if the CTE of the BGO and the load carrying wrapping material are not matched very well. Due to the brittleness of BGO crystals and the poor adhesive strength of optically transparent glue, the necessity of a stiff support structure is given which has to be at least as stiff as the BGO s itself. A simple wrapping, especially of the thin upper ring crystals, by a soft composite shell does not resist the acting loads with sufficient margin of safety. Fracture critical bending of the crystals or breakage of the edges is possible. Therefore, a lightweight but very stiff sandwich-support structure was designed identical for all crystals to reduce the existing bending of the BGO housing (cover plates). Additionally, the gaps between the crystals are minimized reducing the active and passive shield leakage. However, this support structure still shows displacements which results in very critical glue and crystal stresses. Therefore, a decoupling between the crystals and the support structure is necessary. To reduce the torsion and bending stresses, the 2 - 4 subcrystals are attached to each other with an optically transparent, but flexible and elastic already space qualified glue, replacing the previously proposed stiff glue and acting as flexible joint. At the same time, each smaller subcrystal has an isostatic suspension with three bearing pads at the large surfaces and two pads at the small surfaces as shown in Figure 1. These bearing pads (height approx. 0.1 mm) are manufactured from silicon or the soft glue used for subcrystal bonding.

An optional solution for the very thick Side and Rear Shield crystals would be to use monolithic large BGO crystals which can now be drawn by Crismatec (F). Calculations showed that the margin of safety in combination with the proposed BGO suspension is ≥ 15 exceeding conservative safety factor of 10 for brittle materials sufficiently.

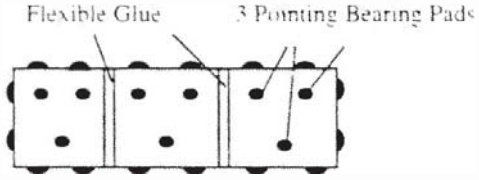

Fig. 1: Large BGO crystal assembled of 3 small subcrystals with flexible glue and isostatic bearing pads

The CTE of the composite sandwich structure manufactured from a CFRP GFRP mixture will be adjusted almost to the one of the crystals (7 -10 K) and of the outer structure. Figure 2 shows a complete crystal support structure.

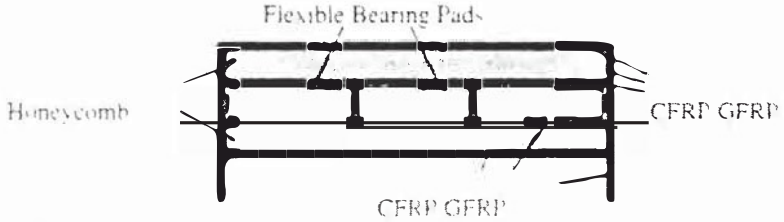

Fig. 2: BGO Crystal Housing (schematic, pads not on scale)

NASTRAN FEM analyses of the most critical detector units of the UCR (Upper Collimator Ring), comprising 3 elastically glued BGO-subcrystals supported through isostatic pads in the composite sandwich structure have been performed under the load of quasistatic accelerations acting in each direction separately. Thus, the results demonstrate the feasibility of the proposed BGO-Crystal suspension design to survive a quasistatic design load of 35g. The results of the three design load cases are shown in the following Table 1.

Table 1: Maximum Displacements and stresses (v. Mises)

Load Case	35g - X		35g - Y		35g - Z	
Total displacement / Stresses	Δxyz	$\sigma_{v.M.}$ [N mm^{-2}]	Δxyz	$\sigma_{v.M.}$ [N mm^{-2}]	Δxyz	$\sigma_{v.M.}$ [N mm^{-2}]
BGO	16.1	0.5	19.6	0.7	21.0	1.1
CFRP-Box	11.9	0.6	14.7	1.8	17.1	5.3

The stresses in the flexible glue are negligible. The resulting maximum displacements and stresses are low compared to the materials allowables (BGO: 130 N mm^{-2}) highlighting the high confidence to the proposed design.

The complete Rear Shield previously designed as one single block with an expensive Titanium structure is very uncomfortable for handling and crystal replacement. Therefore, mechanically decoupled detector modules form the plane and tilted part of the Rear Shield. The complete ACS structure with the stand alone rings is shown in Figure 3.

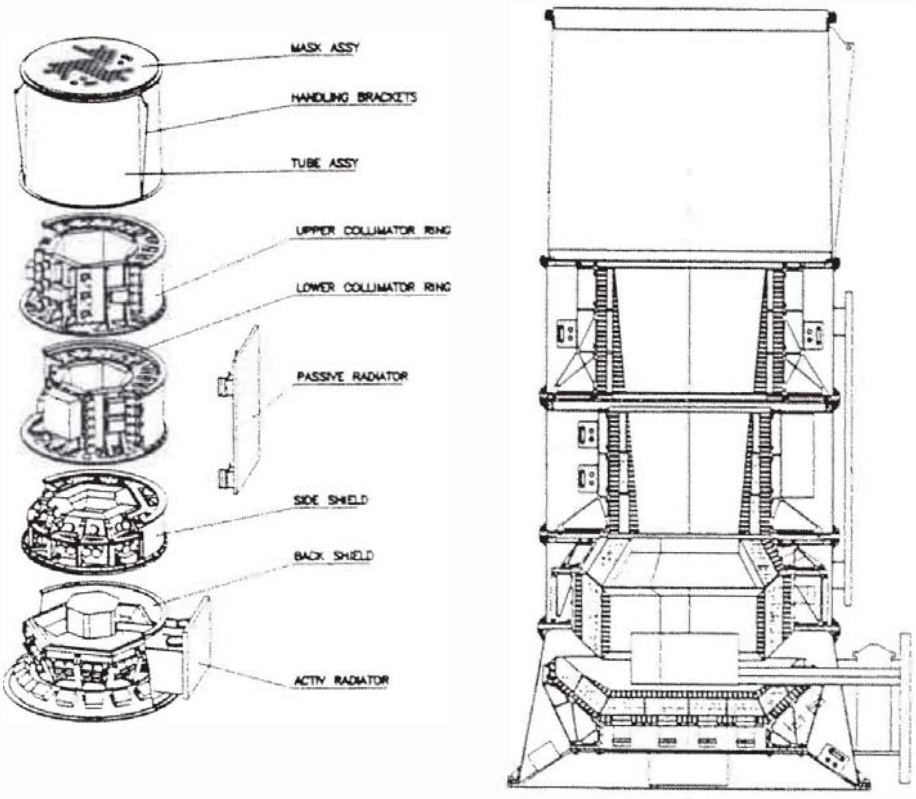

Fig. 3: Complete ACS structure

Detailed structural analyses as mass properties, natural mode, composite and strength (e.g. tube buckling, interfaces) analyses have been performed to verify the structural integrity of our mechanical concept and the stiffness requirements (37 Hz lateral, 75 Hz axial). The computed fundamental frequencies showed a good margin. Generally, the stress levels are moderate, offering some further mass saving potential.

The thermal analyses show that the most critical mode appears for the hot case with a high PLM interface temperature inducing too high temperatures up to about 48°C in the BGO crystals, which are out of limits (approx. 30° C) due to functional reasons (light yield). The integration of an additional radiator, e.g. second surface mirror, should be evaluated to lower the temperature level inside the ACS.

2.2 -Shield Performance

Numerous low energetic gamma-ray photons (50 keV-150 keV) trigger the ACS even if the transmission through the shield for those events is equal to 0. The integration of an extra lightweight shield (30 kg) consisting of 0.5 mm Pb, 0.1 mm Ta, and 0.4 mm Sn (tbc) fastened on the outside of the BGO will reduce the count rates of the X- and low energy gamma-rays by blocking of those events. Thus, the dead time for the ACS and background in the Ge detectors can be clearly reduced. The supplementary mass of the extra shield can be easily compensated by our in general "lightweight" ACS concept.

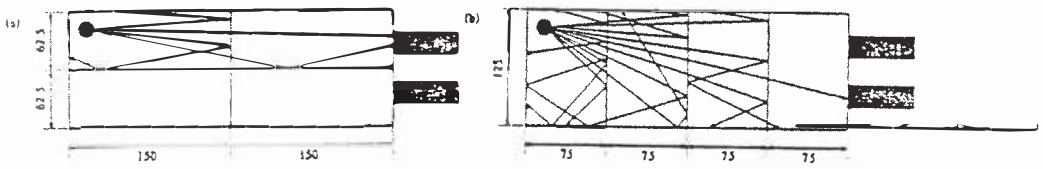

Fig. 4: Possible arrangements (a) & (b) of single BGO plates forming a BGO segment. The segment dimensions were 300x125x20 mm . 4 BGO plates form 1 segment

Each detector unit consists of 2 - 4 glued BGO subcrystals forming the characteristic shield segments. The refractive index of the used glue gives for the scintillation photons a total reflection angle between the BGO plates starting from 41.6° vs the surface normal and so only photons within a solid angle of 1.58 sr pass the glued interfaces. As MC simulations showed, there is no influence of highly transparent glue on the light output. Due to multi-reflection and absorption effects the LCE (Light Collection Efficiency) of the 2 PMTs of each crystal segment is different depending on the location of the scintillation event. As a further result of those MC simulations, the arrangement of the BGO plates as shown in Fig. 4(a) for the gluing of 4 crystal plates is favored because the light passes less transitions of different refractive indices before it reaches the PMT window. The diffuse reflector coating of BGO crystal is strongly determining LCE performance of the detector units as dedicated experimental investigation have shown. The scintillation light in a glued BGO segment is usually several times reflected by the crystal coatings before it reaches the PMT window (compare Fig. 4). Therefore, white diffuser paper will be needed having an absorption coefficient between 1.5% and 2 % promising relevant advantages compared to Teflon (absorbtion coefficient about 5%). *An improvement of 1% in the absorption coefficient leads to an improvement of about 4% absolute in the LCE!* Here, with that improvement due to a rise of all LCE's by about 10% absolute, it can be expected that the required output of 5 P.E. 80 keV gamma-ray energy [2] can be surpassed even for unfavorable gamma ray locations in the BGO segments. Further, a high LCE output level provides high functional reliability even in the case of

BGO degradation through radiation induced damages during mission life time. To reach a status with BGO segments having homogeneous outer dimensions independent from tolerances induced through the coating, a technique relying on the air free filling of the pores of the coating with a vacuum impregnation (EPOFIX) could be used.

For the PMT's a modified version of the 1.5 inch EMI Thorn 517 D was selected. Critical aspects as minimized after trigger behavior due to bulb vacuum impurities, reduced saturation effects due to local overheating effects in the bulb cathodes, and the gain stability were evaluated. Using the SAX experience, a shield shut down (HV power switch-off) in case of the detection of a high energetic particle accelerating the degradation of the PMT's can be easily realized. The moderate PMT performance degradation monitored during one year mission life time of SAX will be matched by adjustable thresholds.

In Table 2 the transmission length for two exemplary Ge detector positions (center and edge) in combination with the affiliated solid angle of the different shield elements (4π - FOV in %) are shown. The requirements 50 mm BGO transmission length is not fulfilled for the Upper Collimator Ring for edge and center detectors and for the Lower Collimator Ring for the edge detectors. But due to the low contribution in terms of solid angle, the impact on the shield performance seems uncritical.

Table 2: Transmission length for the ACS

Description	Solid Angle in %		Loss Solid Angle in % - unshielded sections		Solid Angle in % with less than 50 mm BGO transm.		Minimum Transmission length on average in mm for solid angles with less than 50 mm transmission	
Detector Position	Edge	Center	Edge	Center	Edge	Center	Edge	Center
Upper Collimator Ring	1.6	1.6	-	-	0.18	0.16	31	46
Lower Collimator Ring	6.5	6.5	-	-	2.08	1.68	34	50
Side Shield	63	62	2.19	2.77	2.87	5.19	>44	>46
Rear Shield	27	27	0.07	0.40	0.29	-	>49	-
Total	**98**	**97**	**1.6**	**2.6**	**5.4**	**7**	-	-

The gaps between the different rings, shields and the BGO crystals are responsible for a partial or 'zero' transmission length shield leakage which is in total 2.56% and 1.59% of the solid angle for center and edge detectors. For the most sensitive area, i.e. the Side Shields the leakage in the active shield was improved to 1.3% and 1.5% for center edge detectors. However, all gaps between the crystals are completely closed by approx. 50-100 mm passive composite material.

2.3 - Electrical Subsystem

The following functional performance features for the ACS electronic system are emphasized:

- The ACS electronics shall provide a VETO strobe to the instrument DPE: the VETO is generated starting from individual signals from the PMTs. The anode signals from two PMTs looking into different crystal segments are merged (twin PMT concept).
- Redundancy concept is based on the following rule: no single failure point shall exist that could cause the loss of veto signal from a crystal. Since most of the crystals are viewed by two PMTs, the above concept leads to merge the PMT signals in such a way that a single point failure could affect only one PMT per crystal.

- To provide an optimum of reliability and timing of the VETO signal two different CSA output thresholds are used. The VETO signal shall be generated if the CSA output exceeds the energy trigger threshold but it shall be time related to the exceeding of the event trigger threshold. The over-all delay of the VETO signal is less than 1 μs with a channel-to-channel accuracy of < 15 ns and a noise threshold jitter of < ± 20 ns.
- The VETO duration shall be 350 ± 18 ns for energies of E < 200 MeV and 10 ± 1 μs for energies of E ≥ 200 MeV. Optionally, a further discriminator generating a VETO puls duration of 150 ns ± 8 ns for energies between 150 keV and 200 MeV should be generated.
- The "off the shelf" design follows the space proven SAX -PMT detection chain, electronic, and software design. Thus, an accurate prediction of the operational power consumption (<53 W) and of the performance was a simple and reliable issue.

2.3.1 - Electrical Architecture

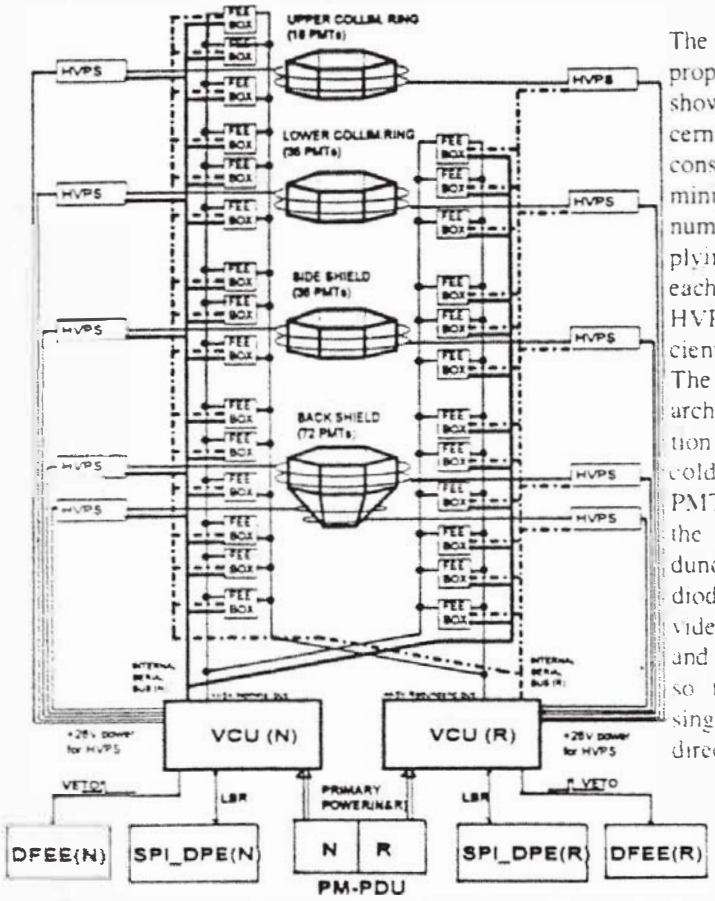

Fig. 5: ACS electronic architecture (electronic boxes, power distribution, Internal Serial Bus, VETO strobes and PHA lines are not shown)

The leading factor for the proposed architecture, shown in Figure 5, concerns the critical power consumption, which was minimized by a reduced number of HVPSs supplying up to 36 PMTs each. Five nominal HVPS boxes are sufficient for the whole ACS. The key of this electrical architecture is the adoption of two HV buses in cold redundancy. Each PMT is supplied by both the nominal and the redundant HV bus that are diode OR-ed at the divider level. The HVPS and dividers are designed so that in case of any single-point failure (e.g. direct HV to GND shorts, anode to cathode short) at divider or PMT level, the HVPS will continue to supply the correct HV to the remaining PMTs. Each HVPS output High-Voltage will be moreover programmable and switchable under telecommand.

2.3.2 - FEE Chains

The FEE concept is based on a splitting between the first level FEE (Charge preamplifier with ancillary circuits) and second level FEE (threshold discriminators, VETO strobe logic, delay lines, equalizer and so on). As baseline the first level FEE is placed on the divider board inside the PMT housing. With the above approach the signal exits the PMT housing as an amplified voltage pulse that is much more easy to deal with than the PMT anodic charge pulse which must be conducted over partly long signal lines.

The second level FEE will be distributed between 27 FEE boxes each one managing the signals coming from 6 PMTs (compare Fig. 6). As the failure of a FEE box will cause the loss of 6 PMTs, the PMT-FEE box assignment shall be done in such a way that PMT signals from the same crystal are routed to two different FEE boxes in order to have a FEE box redundancy on each crystal.

The logic block is devoted to the Veto generation (one Veto signal as "OR" of the three Vetos from the three couples of PMTs) with the required timing relationship for the incoming PMT signals. This block includes all the delay lines and delay equalizer being adjustable on-ground.

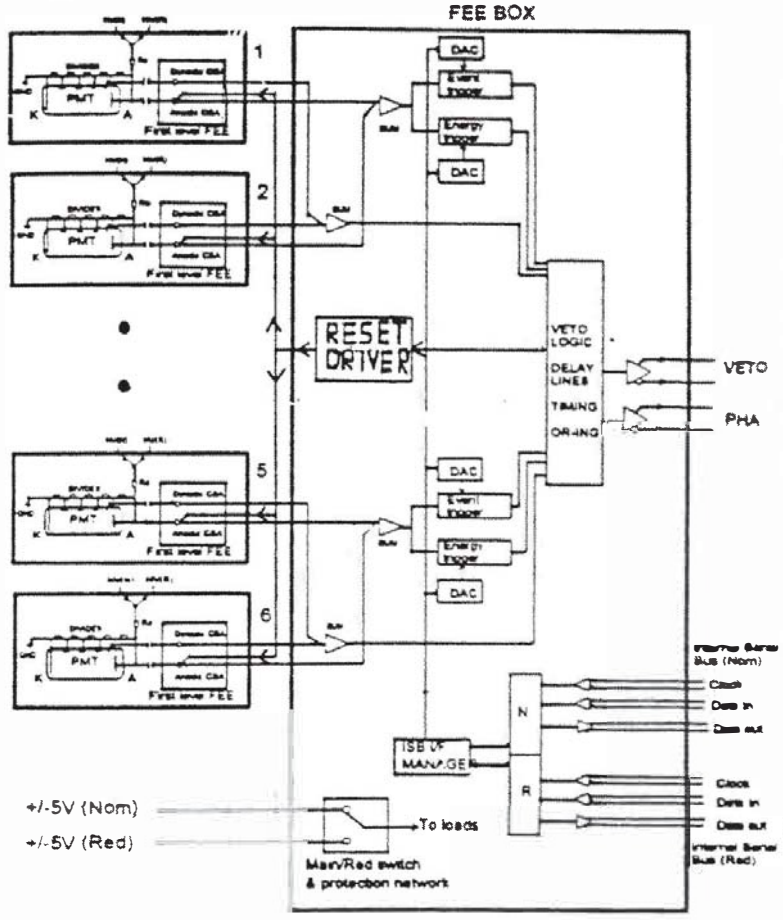

Each FEE and HVPS box is linked to redundant inter-nal serial (party-line) synchronous buses (ISB) mastered by the VCU for command and housekeeping reception transmission. Proper splitting into four (TBC) multiplexed ISB segments are foreseen in order to match bus drivers loading requirements. The communication protocol on the ISB bus is identical to the

Fig. 6: FEE concept: first level FEE and FEE box serving six PMTs

INTEGRAL IBIS constellation. The VETO and PHA signals is routed to the VCU units via 422-like differential interfaces.

2.3.3 - Veto Control Unit

Each SPI ACS Veto Control Unit (VCU) will provide a regulated low voltage power bus to supply the FEE and HVPS boxes, collect the VETO strobes PHA pulses, generate a single VETO strobe ("OR" sum of all the FEE-level strobes) and a PHA spectra, and manage the interface TM/TC. The block diagram of the VCU is shown in Figure 7.

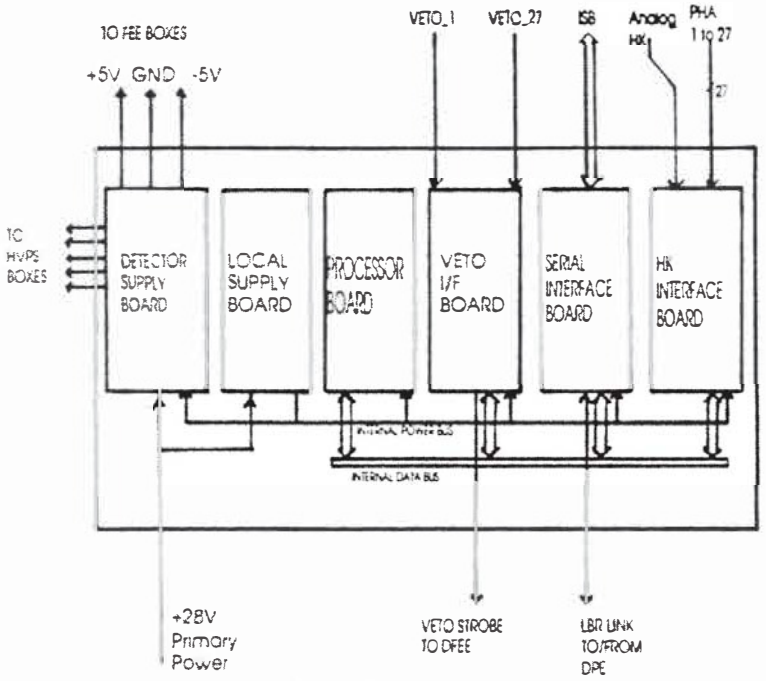

Fig. 7: VCU block diagram

2.3.4 - Timing Description

In the following a simplified timing for the VETO generation related to a signal in the 80 keV to 2 MeV energy window is described. Starting event is the arrival of a photon in the shield. The related anode signal is collected by the FEE and put at the comparators input. After a short delay (To) the first threshold (Event threshold, Eo) is crossed and a signal is generated at the output of the Event Trigger. A trade-off has to be made between the Event threshold level and the maximum allowable walk-time jitter of To. Further, a second signal is generated when the second threshold (Energy threshold, E1) is crossed.

The Event Trigger Output signal is individually delayed through a passive delay line having 600 ns + - 15 ns nominal delay (T1). The T1 delay (called integration time) is adjustable within + - 15 ns in the 600 to 650 ns range for the FEE box equalization purpose in order to compensate for the different device and harness dependent delays of the various signal chains. If the delayed Event Trigger becomes active then a FEE-internal "Start signal" is generated. A FEE-internal "Stop signal" is generated after a 350ns + -

5% delay (Tv) from the Start. Here, the Tv delay defines the length of the Veto pulse at the FEE box output.

In case of an overrange situation (energies above 200 MeV), a proper circuit will prolong the Tv delay to 10 + - 1 µs. A passive tapped delay line, with the delay (Te) adjustable in 10ns steps between 0 to 100ns is provided for each of the 27 VETO inputs of the VCU. Thus, allowing an equalization of the delays from the various FEE boxes (interface of the FEE box to the VCU). The VETO signal at VCU output is not more than some 50 ns delayed with respect to the above signal. From the description above follows that the longest time from an event arrival at the detector and the generation of the VETO signal at the VCU output is below 1µs. The comparator jitter will be around+ - 10 ns for energies 10 KeV above the selected threshold as far overdrive is concerned.

2.3.5 - Electronics Special Performance Features

Pulse Height Analyses (PHA)

For diagnostic and spectrometric (PHA) purposes, a 128 channel x 16 bit multichannel analysator with a linear (within + - 2%) relationship between anode charge and channel number was implemented. A PHA pulse is generated with a pulse length, linearly proportional to the anode signal amplitude. The pulse duration will range from 1 to 32 µs for energies between 80 keV and 2MeV and up to 40 µs for higher energies or overlapping (piled-up) pulses. Only the pulses above the energy threshold will be processed by PHA and all PHA signals from the FEE boxes are collected by the VCU (HK interface board). At the VCU, they will be multiplexed to the input of a time measurement circuit based on a 128 bit counter running at 4MHz. For each pulse the result of the time length measurement (7 bit number) will be used to address one (out of 128) 16bit memory which contents is to be incremented by one. All the PMTs are sequentially read out with 10 minutes data accumulation each and the individual spectra data are stored in the VCU RAM.

PMT Test Generators

On-flight diagnostic of the ACS can be made by means of the ratemeter function or the PHA function using natural (e.g. background radiation) sources. Additionally on board pulse generators in each FEE box as standard signal sources for on-flight diagnostics are implemented, actuated by TC. It is composed by a multivibrator generating voltage pulses of duration 1µs + -10% (TBC) and 500 Hz + - 20 % (TBC) repetition rate. The output of the multivibrator drives a LED placed in proper position in the field of view of the channel related PMT. The LED intensity is matched with the LED+PMT optical coupling characteristics.

Dynamic Blocking Time

The scintillation detectors with PMT's have the behavior to generate after-pulses in case of an excitation through a higher energy event. This after-pulsing can produce additional Veto signals. Through the integration characteristics of the CSA and the necessary time of the CSA-output voltage returning to the baseline after the generation of a Veto signal, an energy dependent blocking time is introduced into the electronic circuit of a BGO segment. Assuming crystal segment count rates of 1000 cnts s, for a blocking time of 5 µs the average probability for particles passing the shield undetected is only about 0.5%.

3 - CONCLUSIONS

The following benefits can be highlighted for future functionally, electrically and structurally improved ACS concepts:

- Significantly improved Light Collection Efficiency lowers threshold level and provides good margin against life time radiation damages
- Simple aluminum turning/grinding items and low manufacturing tolerance requirements reduce procurement costs
- Easy and quick crystal replacement and repair of all crystal segments within one week feasible
- Structurally optimized BGO suspension and unambiguously arranged load paths avoiding stress peaks and large displacements in the BGO crystals
- "Off the shelf equipment as flight proven SAX electronics (H/W, S/W) with reliable power figures and procurement schedule minimizing costs and risks.
- Future technologies for scintillation detectors using different crystal materials in combination with photodiode detectors promising different improvements and advanced scientific applications [3] - [5].

4 - ACKNOWLEDGEMENTS

We would like to express special thanks to Dr. Schwenkenbecker and Dr. Göbel, Crystal GmbH for their expertise in BGO scintillation technology.

The study activities were funded by Kayser-Threde, LABEN and CASE.

5 - REFERENCES

[1] E. Alippi, A. Lenti, F. Monzani et al "The X-ray instruments and future of X-ray astronomy from SAX" from "Symposium on Sientific Satellites Achievements and Prospects in Europe 20-22 Nov. - Paris-France

[2] R. Georgii et al.." Optimization of the veto shield for the INTEGRAL spectrometer SPI with Monte Carlo simulations' R. Georgii et al., *SPIE-Proceedings*, Denver, 1996

[3] R. Graue, T. Stuffler, T. Göbel, "A compact Gamma Ray Detection System for Space Applications based on Photodiodes and CsI (Tl) Scintillation Crystals;" *SPIE Proceedings*, Denver, 1996.

[4] R. Graue, T. Stuffler, T. Göbel, K. Schwenkenbecker, "High Resolution-Gamma Ray Detection System for INTEGRAL, *AAAF-ESA-Scientific Satellites Achievements and Prospects in Europe*, 1996".

[5] T. Stuffler, R. Graue, A.J. Bird, A.J. Dean, R. Staubert, "PIMACS (Polarimeter and Improved Modular Anti-Coincidence System) an effective instrument concept for X-, Gamma-ray monitoring, and polarimetry measurements on the International Space Station", *ICSO Symposium*, Toulouse,1997.